CHEMICAL ENGINEERING TRANSACTIONS
VOL. 67, 2018
A publication of AIDIC
The Italian Association of Chemical Engineering
Online at www.aidic.it/cet
Guest Editors: Valerio Cozzani, Bruno Fabiano, Davide Manca

ISBN 978-88-95608-64-8; **ISSN** 2283-9216

CFD Study of the Behavior of LPG Tanks Exposed to Forest Fires

Giordano E. Scarponi[a,*], Frederic Heymes[b,]

[a]LISES - Dipartimento di Ingegneria Civile, Chimica, Ambientale e dei Materiali, Alma Mater Studiorum - Università di Bologna, via Terracini n.28, 40131 Bologna, Italy.
[b]Ecole des Mines d'Ales, 30319 Alès (France)
giordano.scarponi2@unibo.it

Forest fires represent a growing safety concern since their frequency is increasing, with severe damages to humans, environment and structures. The present work focuses on the impact of forest fires on a particular type of target: liquefied petroleum gas (LPG) tanks. A computational fluid dynamic (CFD) model was applied to simulate the response of LPG tanks of different sizes exposed to a forest fire scenario. Results are presented in terms of pressurization rates, temperature distributions and velocity fields focusing on the effects of the tank size variation on the vessel response. In particular, it is pointed out how the tank diameter greatly affects the pressurization rate, but it as a negligible effect on the wall temperature distribution. The outcomes of this work provide useful results to evaluate the possible failure conditions, thus supporting the emergency response to wildland fires.

1. Introduction

Forest fires represent a potential treat for humans, civil structures and industrial facilities as well as for the environment (Argañaraz et al., 2017). The concern related to this kind of accidental scenario is growing. In fact, the global warming increases the occurrence frequency of extreme fires (Dimitrakopoulos et al., 2011). Furthermore, the fast urbanization leads to the spread of the Wildland-Urban Interface, leading to increment of ignition sources and consequent impact of wildfires on neighboring structures and people (Rossi et al., 2011). Therefore, investigating the safety-related aspects of the interaction of forest fires with wildland-urban interface elements is of utmost importance for effective emergency response planning and preparedness (Heymes et al., 2013a). The present work focuses on the impact of forest fires on a particular type of target: LPG (liquefied petroleum gas) tanks of different scales. Especially in rural areas, LPG is commonly adopted for domestic use and above-ground storage tanks are located outside of houses, often in the proximity of forests. When exposed to a severe heat load induced by fire, LPG tanks heat-up and pressurize (D'Aulisa et al. 2014). This may lead to the catastrophic tank failure, which, in turn, may be followed by dangerous events, such as boiling liquid expanding vapour explosion (Landucci et al. 2013), fireball (Landucci et al., 2015) and missiles projection (Tugnoli et al., 2014). These events may severely affect people and structures in the proximity of the tank, worsening the effects associated with wildfires (Maillette and Birk, 1996). In order to characterize and predict the response of LPG tanks exposed to forest fire scenarios, Scarponi et al. (2018) proposed a two-dimensional (2D) model, based on computational fluid dynamic (CFD). This was validated against data from a fire test simulating a forest fire scenario. The model predictions showed a good agreement with the experimental measurements in terms of pressure and temperatures, but the application to multiple geometrical configurations of LPG tanks was lacking. In the present work, the model is extended to simulate the exposure of different LPG tanks types to a forest fire scenario, with the aim of studying the influence of the tank geometry on the vessel response.

2. Overview of the modelling approach

2.1 Model equations

The CFD model used in the present work solves the governing equations for mass, momentum and energy throughout the computational domain. Two additional equations for the conservation of the turbulence kinetic energy and dissipation rate are also included. All the simulations, carried out using the software ANSYS® Fluent® 18.2.0, considered a 2D vertical (and perpendicular to the axial direction) section of cylindrical tank positioned horizontally (see Figure 1). The Volume Of Fluid (VOF) (Hirt and Nichols, 1981) was selected as multiphase model. This is suitable when two or more immiscible phases are present. It tracks the interface between the phases by solving a continuity equation for the volume fraction of one (or more) of the phases. In the problem considered here, two phases are present: the liquid (*L*) and the vapor (*V*). The latter one was chosen as the primary phase to avoid convergence problems. In this case, the continuity equation for the liquid volume fraction (α_L) is expressed according to Eq(1), where ρ_L is the density of the liquid and $\vec{u}$ is the velocity, which is shared by the two phases. The volume fraction of the vapor phase is then obtained from the liquid volume fraction considering that, in each cell, they must sum to 1.

$$\frac{\partial}{\partial t}(\alpha_L \rho_L) + \nabla \cdot (\alpha_L \rho_L \vec{u}) = m_{L\to V} - m_{V\to L} \quad (1)$$

$$m_{L\to V} = C_E \alpha_L \rho_L \left(\frac{T - T_{sat}}{T_{sat}}\right) \quad (2)$$

$$m_{V\to L} = C_C \alpha_V \rho_V \left(\frac{T_{sat} - T}{T_{sat}}\right) \quad (3)$$

The terms $m_{V\to L}$ and $m_{L\to V}$ represent the mass transfer rate from the vapor phase to the liquid one (condensation) and vice-versa (evaporation). They were defined according to the evaporation-condensation model implemented in ANSYS® Fluent® and based on the work of Hertz-Knudsen (Knudsen, 1934). In a given cell of the computational domain, evaporation will occur when the temperature is above the saturation temperature (calculated at the cell pressure) according to Eq(2), where T is the cell temperature; T_{sat} is cell saturation temperature. On the contrary, when the cell temperature is below the saturation temperature, part of the cell content will condense according to Eq(3). The coefficients C_E and C_C are both set to the default value of 0.1 s^{-1}, in accordance with guidance reported elsewhere (Landucci et al., 2016) dealing with liquid-vapor LPG systems. According to several authors that studied the response of LPG vessels exposed to fire, the flow regime both in the liquid and the vapor space can be considered turbulent. Therefore, a turbulence model was needed for the present analysis. In particular, the k-ω SST (Launder and Spalding, 1972) was selected, as proposed by Scarponi et al. (2018). This model can be integrated throughout the boundary layer avoiding the use of wall functions. Details on the complete set governing equations adopted in the present work can be found in Scarponi et al. (2018).

Fluid properties (pure propane was considered in all simulations) are expressed as a function of temperature according to thermodynamic data provided in Liley et al. (1999). The Soave-Redlich-Kwong state equation was considered to be valid for the vapor phase. The thermal properties of carbon steel for the tank wall were taken from (CEN, 1998). All the simulations were run for 1200s.

2.2 Solution methods

A first order implicit scheme was adopted for the transient formulation, with a timestep of 5 ms. A second order upwind scheme was chosen for the spatial discretization of density, momentum, energy and turbulent quantities (k and ω), whereas the PRESTO! and the Geo-Reconstruction schemes were used for the pressure and the volume fraction respectively (ANSYS inc, 2012). Pressure and velocity coupling was obtained by means of the SIMPLEC (Semi-Implicit Method for Pressure Linked Equations-Consistent) algorithm. At each time step, the solution was considered converged when one of the following criteria was satisfied:

- The sum of the scaled residuals was below 10^{-3}
- For a given time step, the ratio between the residuals and the residuals at the beginning of the time step was below 0.05

2.3 Case study definition

In order to study the effect of the tank dimension on pressurization rate, temperature distributions and physical phenomena characterizing the vessel response to fire exposure, three different case study were defined as reported in Table 1. The same thickness was considered for all the tanks in order to exclude the effects of this parameter in the comparison of the results obtained in the different cases. This would have the effect of delaying the tank pressurization and keeping the tank wall colder. In all the cases, the 80 % of the tank volume was considered to be occupied by the liquid phase.

Table 1: Case study definition

Case	Tank diameter (m)	Number of mesh cells
Case 1	1.0	153,272
Case 2	1.6	312,713
Case 3	2.2	503,413

2.4 Fire scenario and boundary conditions

The scenario taken into consideration is a 100 m wide by 40 m high fire front with an average emissive power of 90 kW/m^2. This was taken as reference scenario in the study of the impact of a distant wildland fire on an LPG tank by Heymes et al. (2013b). For all the three cases listed in Table 1, a distance of 50 m was assumed between the fire front and the tank center. The amount of heat radiation (I_P) hitting a given point (P) on the tank wall can be expressed (neglecting the radiation absorbed by the air) according to Eq(4a), where $T_{F,BB}$ is the equivalent black body temperature of the fire, σ is the Stefan-Boltzmann constant, T_∞ is the temperature of the surrounding and $f_{P\to F}$ is the view factor between point P and the fire.

$$I_P = \sigma \times \zeta \tag{4a}$$

$$\zeta = f_{P\to F} {T_{F,BB}}^4 + (1 - f_{P\to F}) {T_\infty}^4 \tag{4b}$$

$$q(\theta, t) = \sigma \varepsilon_w \left(T_{BB,eq}(\theta)^4 - T_w(t)^4 \right) \tag{5}$$

The CFD simulation considered the tank 2D section identified by the green plane depicted in Figure 1b (i.e. a vertical plane cutting the tank in the middle). However, the view factors between each point of the tank external wall and the fire where calculated considering the three dimensional geometry schematized in Figure 1b. The values of the view factors as a function angle θ (see Figure 1a, showing also the incident radiation I_P) obtained for the three cases listed in Table 1 are very similar to one another. This is due to the small variation of the tank diameter with respect to the dimension d, L and H characterizing the fire scenario.

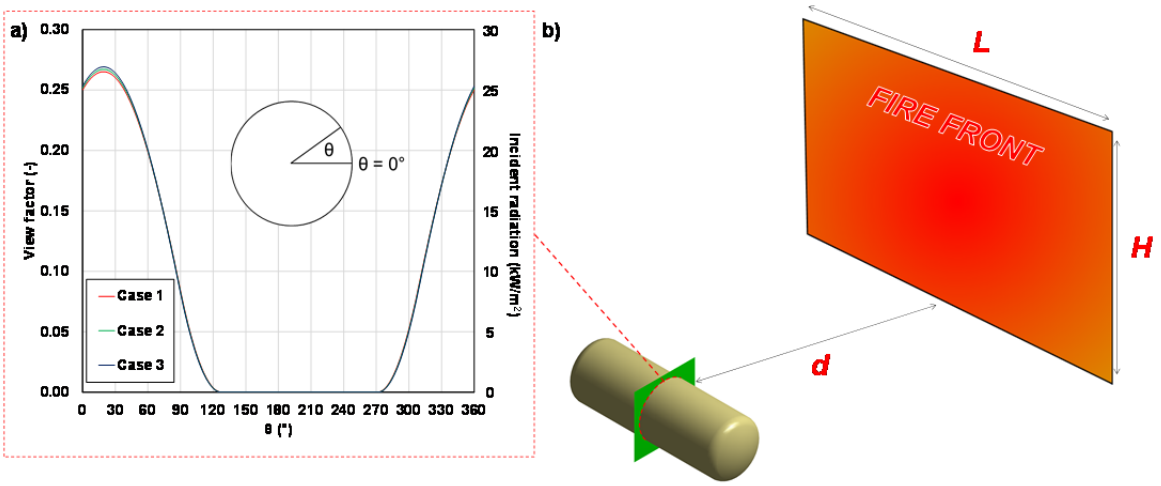

Figure 1: Values of the view factors as a function angle θ obtained for the different case studies (a) and schematic representation of the tank exposure to a forest fire front (b).

The solver calculates the entering heat flux (q) for each point at the external wall according to Eq(5), where ε_w is the wall emissivity (ε_w = 0.77 was used in all the simulations) and T_w is the temperature of a given point at the external tank wall. The heat flux is a function of time (the wall temperature changes during the calculation) and the angle θ as defined in Figure 1a. At the beginning of the simulations, the tank lading was assumed to be motionless and at the saturation pressure at 20°C. Turbulent kinetic energy and specific dissipation rate were initialized at 10^{-9} m^2/s^2 and 10^{-3} s^{-1} respectively. The No-slip condition was set at the inner wall.

2.5 Mesh definition

The computational grid was obtained using ANSYS® Meshing™ and is formed by a combination of quadrilateral and triangular elements, resulting in an unstructured mesh. For all the cases, regardless of the tank diameter, the maximum cell size was 3.3 mm with a global growth rate of 1.2. The inner and the outer wall were divided in the same number of segments, so that each segment on the outer wall was approximately 1mm-long. In order to ensure a good resolution in the near wall region, 50 inflation layers were built starting

from the inner wall of the tank with a growth rate of 1.1. The first layer thickness was set to 70 μm. The mentioned parameters were used to build the meshes for the various tanks considered in the case studies listed in Table 1, where the mesh size for the different cases also reported.

3. Results and discussion

When a tank is exposed to fire, the internal pressure rises. This can lead to the tank failure and produce severe consequences due to the sudden expansion of the vessel content. Figure 2 shows that the lower the tank diameter, the higher the pressurization rate. This behavior can be explained considering that the heat flux entering the tank is proportional to the tank area, whereas the thermal capacity is proportional to the tank volume. This means that, for cylindrical tanks of the same length (in 2D simulations this length is infinite) the temperature rise, and therefore the pressure rise, is inversely proportional to the tank diameter.

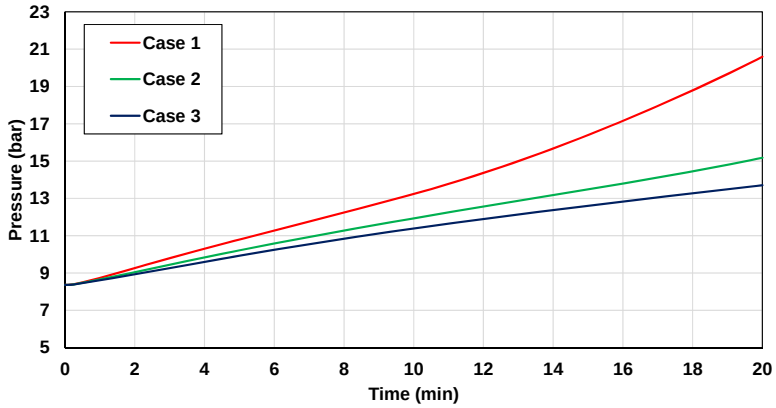

Figure 2: Pressurization curves obtained for the three case studies listed in Table 1.

The pressure rise is not the only factor that can determine the vessel failure. Another critical issue is represented by the degradation of the steel material properties at high temperatures. Figure 3 compares the temperature distributions along the tank wall obtained for the three case studies at different instants of time.

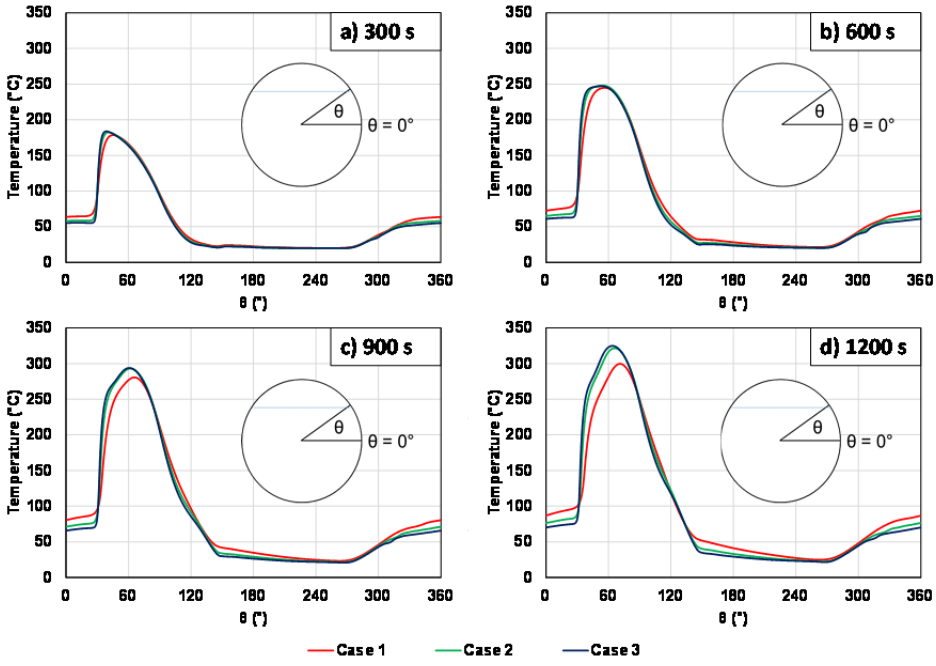

Figure 3: Outer wall temperature profiles at 300 s (a), 600 s (b), 900 s (c) and 1200 s (d) as a function of the angular coordinate θ, defined in Figure 1.

It is clearly visible how the wall below the liquid surface remains quite cold due to the high heat transfer coefficient in the liquid phase. Such behaviour was observed in several fire tests (e.g. Birk et al., 2006). The

liquid wetted wall temperature decreases with the increase of the tank diameter. On the other hand, the wall portion in contact with the vapor experiences a more severe heat-up, but reaching temperatures always far from the thermal weakening limit of low carbon steel (i.e. at temperatures higher than 400 °C (Landucci et al., 2013)). In this region, very similar temperature distributions are registered for all the cases. However, in the second part of the simulations (i.e., after 600 s), the profile related to the smallest tank (case 1) slightly deviates from the other two. This is due to the upwards displacement of the liquid surface, determined by the thermal expansion of the liquid itself. Such phenomenon increases the extension, in terms of the angular coordinate, of the wall portion in contact with the liquid, with consequent enhanced cooling effect.
Figure 4a compares the temperature distributions below the liquid surface obtained for the three case studies after 10 min from the beginning of the simulations. In all the case, the liquid appears to be strongly stratified. Despite the asymmetry of the fire scenario (only the right side of the tank is exposed to fire) the temperature is almost constant in the horizontal direction. On the other hand, the temperature variation along the vertical coordinate is clearly visible, especially in case 1, featuring small tank size. As the tank diameter increases (cases 2 and 3), the liquid bulk remains colder, due to the higher thermal capacity.

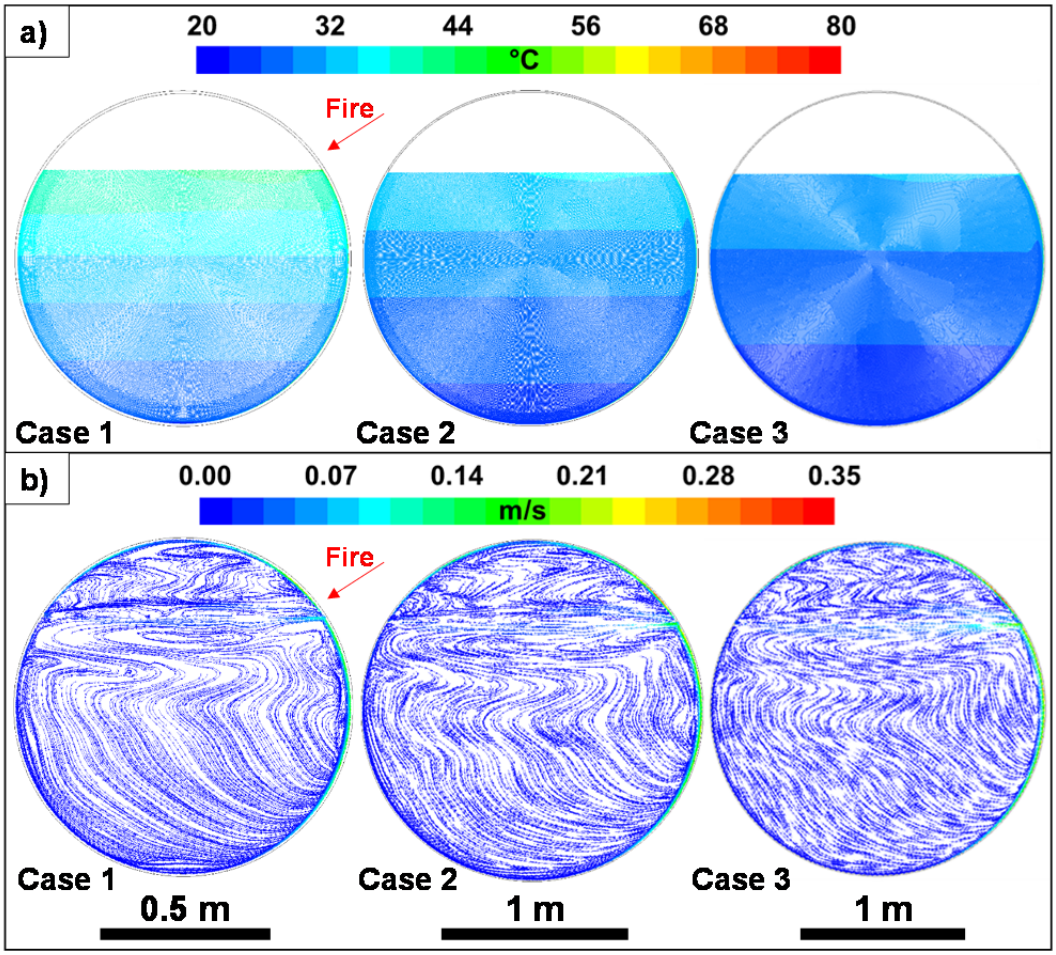

Figure 4: Temperature distribution in the liquid phase (a) and pathlines colored according to the velocity magnitude for the three case studies after 10 min from the beginning of the fire exposure.

Figure 4b shows the pathlines after 10 min from the fire start for the three case studies. A similar behavior can be observed in all of them. The velocity is quite small almost everywhere, except for a free convective layer forming in the region close to the exposed wall (the right side). The thickness of this layer increases with the tank diameter. The liquid rises parallel to the wall up to the surface, proceeds from right to left slowing down, in the direction of the tank vertical centerline and then falls back towards the bulk. It is interesting to note how, in the smallest tank (Case 1), a recirculation cell with an elongated shape forms just below the liquid-vapor interface. A similar behavior can be observed in the second case. Here, however, the center of this cell is closer to the side exposed to fire. This displacement is even more evident in the largest tank (Case 3).
In the vapor space the flow is more chaotic, with several and irregularly shaped recirculation cells forming and disappearing periodically. In this case, the variation of the tank diameter produces no visible effect.

4. Conclusions

The modelling approach presented in this work allowed to study the response of LPG tanks to a forest fire scenario, analysing how the influence of the tank size affects the vessel temperature rise and consequence pressure build-up. It was pointed out that the pressurization rate decreases with the increase of the tank diameter. On the other hand, the tank size as a negligible effect on the wall temperature distribution. In all cases, the model showed that the maximum wall temperature is quite far from critical values at which steel suffers thermal weakening. The liquid is strongly stratified, even though the fire scenario is asymmetric. This behavior was observed in all the case studies, regardless of the tank size. It can be concluded that the CFD model described in this work proved to be a powerful tool to investigate the response of LPG vessels exposed to fire. Simulation results, such as pressurization rate and maximum wall temperature, may be used to evaluate the possible failure conditions due to the thermal weakening of the tank steel structure, thus supporting the emergency response to wildland fires.

References

Alcasena F. J., Salis M., Ager A. A., Arca B., Molina D., Spano D., 2015, Assessing Landscape Scale Wildfire Exposure for Highly Valued Resources in a Mediterranean Area, Environmental Management, 55(5), 1200–1216.

Argañaraz J. P., Radeloff V. C., Bar-Massada A., Gavier-Pizarro G. I., Scavuzzo C. M., Bellis L. M., 2017, Assessing wildfire exposure in the Wildland-Urban Interface area of the mountains of central Argentina, Journal of Environmental Management, 196, 499–510.

Birk A.M., Poirier D., Davison C., 205, On the response of 500 gal propane tanks to a 25%engulfing fire, Journal of Losso preventions in the Process Industries, 19, 527-541

Cardil A., Molina D. M., 2015, Factors Causing Victims of Wildland Fires in Spain (1980–2010), Human and Ecological Risk Assessment: An International Journal, 21(1), 67–80.

CEN - European Committee for Standardization, 1998, EN 10222-1, Steel forgings for pressure purposes. Part 1: General requirements for open die forgings. Brussels, Belgium: European Committee for Standardization.

D'Aulisa A., Simone D., Landucci G., Tugnoli A., Cozzani V., Birk, A.M., 2014, Numerical simulation of tanks containing pressurized gas exposed to accidental fires: Evaluation of the transient heat up, Chemical Engineering Transactions, 36, 241–246.

Dimitrakopoulos A., Gogi C., Stamatelos G., Mitsopoulos I., 2011, Statistical Analysis of the Fire Environment of Large Forest Fires (>1000 ha) in Greece, Polish Journal of Environmental Studies, 20(2), 327–332.

Heymes F., Aprin L., Ayral P. A., Slangen P., Dusserre G., 2013, Impact of Wildfires on LPG Tanks, Chemical Engineering Transactions, 31, 637–642.

Heymes F., Aprin L., Forestier S., Slangen P., Baptiste J., François H., Dusserre G., 2013, Impact of a distant wildland fire on an LPG tank, Fire Safety Journal, 61, 100–107.

Hirt C. W., Nichols B. D., 1981, Volume of fluid (VOF) method for the dynamics of free boundaries, Journal of Computational Physics, 39(1), 201–225.

ANSYS® FLUENT® 14.5, 2012 Theory Guide, Cecil Township, PA: ANSYS Inc.

Knudsen, M., 1934, The kinetic theory of gases. Some modern aspects. London, UK: Methuen and Co., Ltd.

Lampin-Maillet C., Jappiot M., Long M., Morge D., Ferrier J. P., 2009, Characterization and mapping of dwelling types for forest fire prevention, Computers, Environment and Urban Systems, 33(3), 224–232.

Landucci G., Cozzani V., Birk, M., 2013, Heat Radiation Effects, in Reniers, G. and Cozzani, V. Eds., Domino Effects in the Process Industries: Modelling, Prevention and Managing, 70-115

Landucci G., Reniers G., Cozzani V., Salzano E., 2015, Vulnerability of industrial facilities to attacks with improvised explosive devices aimed at triggering domino scenarios, Reliab. Eng. Syst. Saf., 143, 53-62.

Landucci G., D'Aulisa A., Tugnoli A., Cozzani V., Birk A. M., 2016, Modeling heat transfer and pressure build-up in LPG vessels exposed to fires, International Journal of Thermal Sciences, 104, 228–244.

Launder B. E., Spalding D. B., 1972, Lectures in mathematical models of turbulence, London, UK: Academic Press.

Liley P.E., Thomson G.H., Friend D.G., Daubert T.E., Buck E., 1999, Physical and chemical data, Section 2, In Perry's chemical engineers' handbook (7th ed.), New York, NY: McGraw Hill.

Maillette J., Birk, A.M., 1996, Influence of release conditions on bleve fireballs, In American Society of Mechanical Engineers, Pressure Vessels and Piping Division (Publication) PVP, 333, 147–152

Rossi, J. L., Simeoni, A., Moretti, B., Leroy-Cancellieri, V., 2011. An analytical model based on radiative heating for the determination of safety distances for wildland fires. Fire Safety Journal, 46(8), 520–527.

Scarponi G. E., Landucci G., Heymes F., Cozzani V., 2018, Experimental and numerical study of the behavior of LPG tanks exposed to wildland fires, Process Safety and Environmental Protection, 114, 251–270.

Tugnoli A., Gubinelli G., Landucci G., Cozzani V., 2014, Assessment of fragment projection hazard: Probability distributions for the initial direction of fragments, Journal of Hazardous Materials, 279, 418-427.